Sandia National Laboratories

Exceptional service in the national interest

INVESTIGATING MICROSTRUCTURE-PROPERTY RELATIONSHIPS IN TANTALUM ALLOYS

Grant Litynski & Abdelrahman Atef Youssef

Mentors:

Kumar Vemaganti, Hojun Lim, John Shimanek, Jennifer Fort, & Zahra Ghanbari

Presented at the NOMAD XIII Final Presentations on August 4, 2026

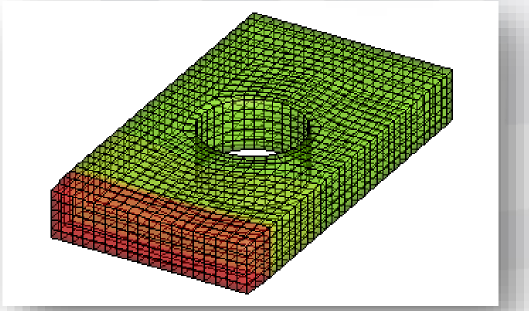

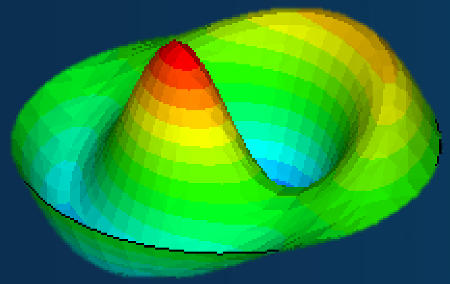

MATLAB > Python

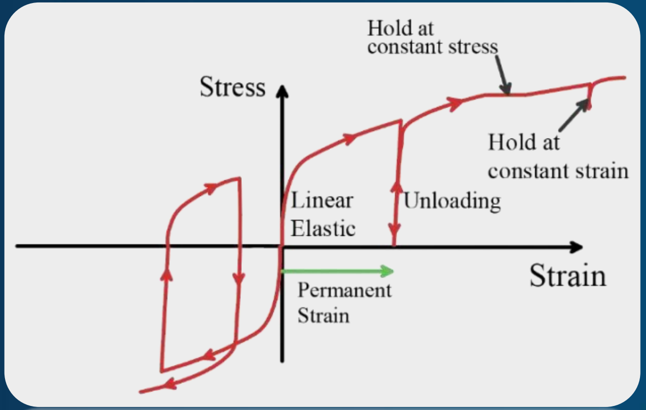

U.S. DEPARTMENT of ENERGY
NNSA
Sandia National Laboratories is a multimission laboratory managed and operated by National Technology & Engineering Solutions of Sandia, LLC, a wholly owned subsidiary of Honeywell International Inc., for the U.S. Department of Energy's National Nuclear Security Administration under contract DE-NA0003525.

SAND2026-24726PE

PROJECT BACKGROUND & GOALS

Goal: Investigate differences in ductility among Ta-10W alloy specimens using macroscale and mesoscale modeling approaches.

Room Temperature Ta-10W Tensile Data

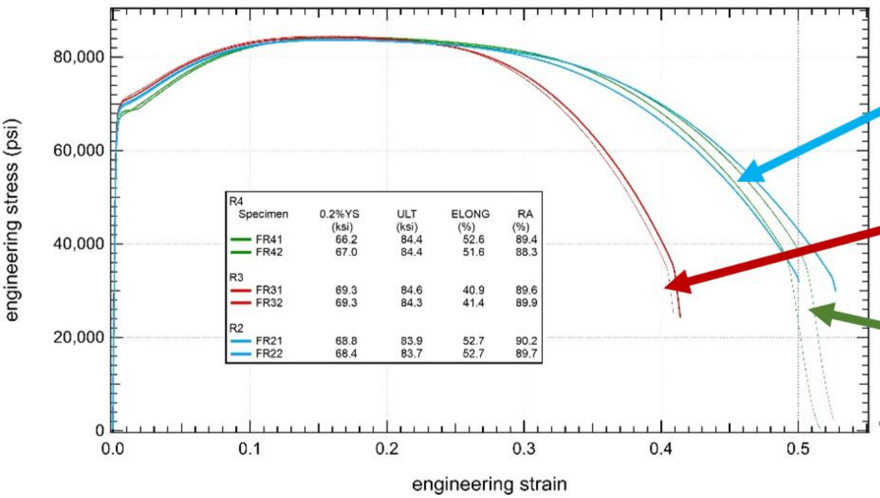

Specimen extraction maps for tensile data shown

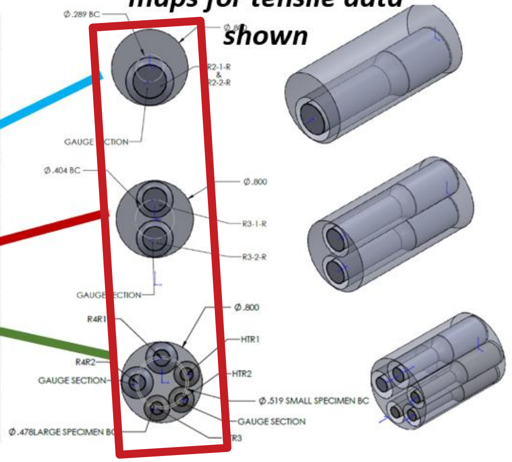

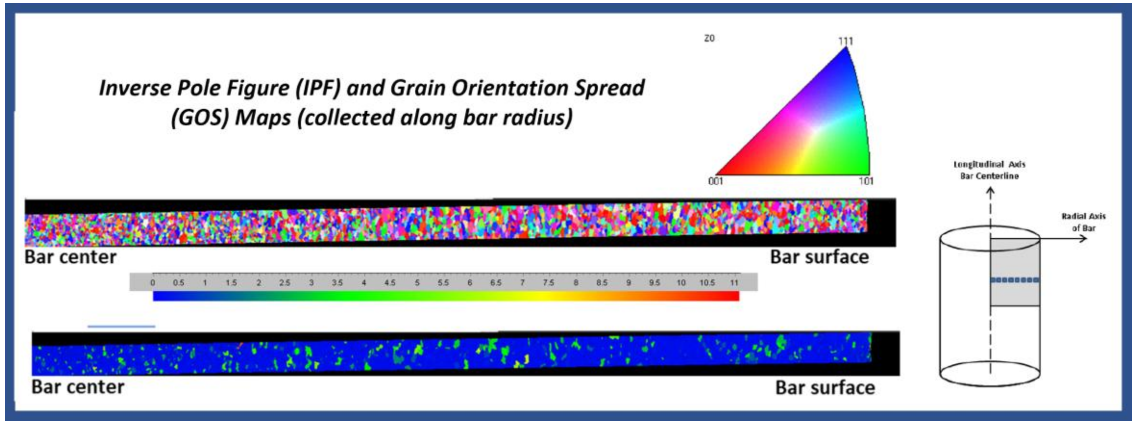

Z. Ghanbari and B. Antoun, SAND2022-7885O

Approach 1: Macroscale (Homogenous)

Approach 2: Mesoscale (Heterogenous)

OBJECTIVES

Experiment Analysis

Macroscale Model

- Metal Plasticity
- Damage

Mesoscale Model

- Computational Microstructure
- Local Damage Variables

EXPERIMENT: DATA ANALYSIS

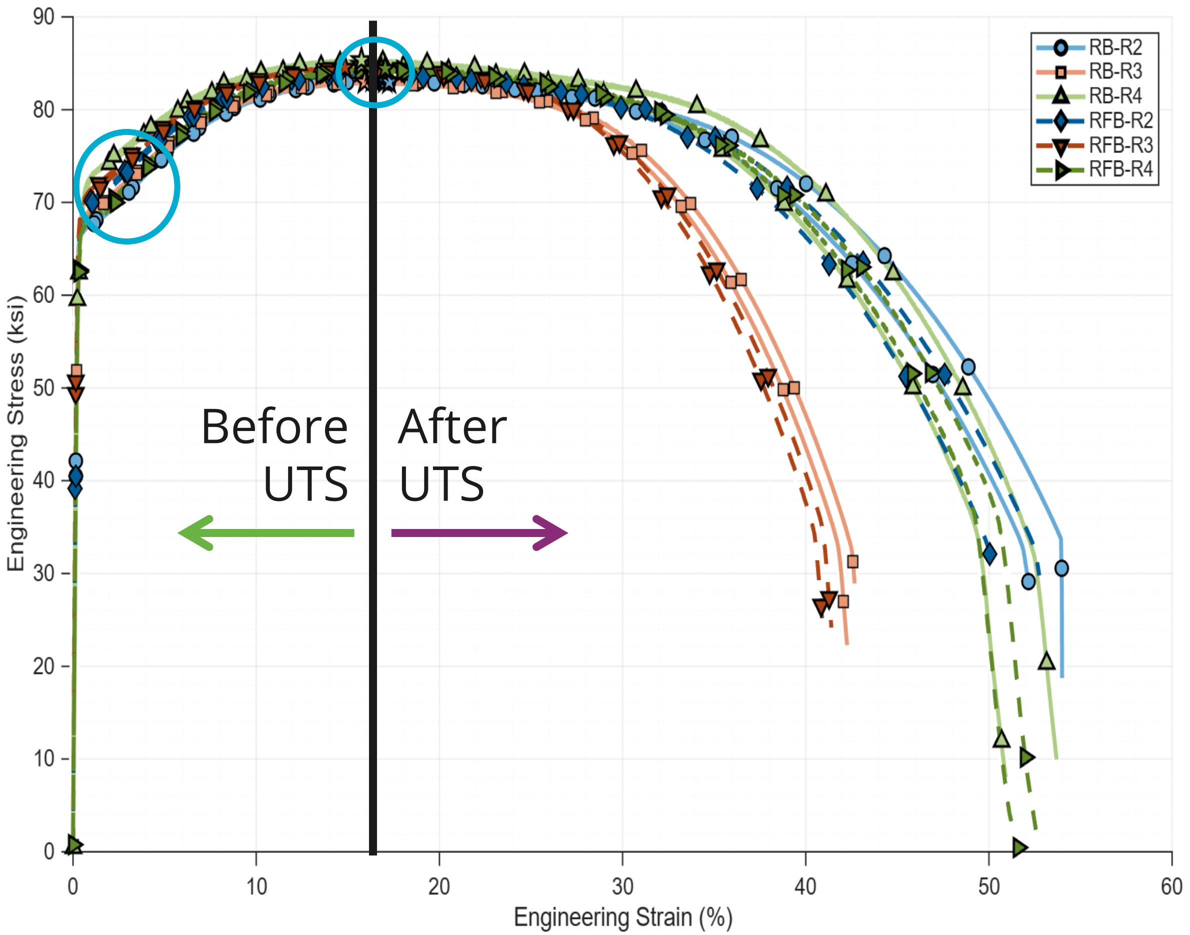

Fig. 1. Experimental tensile data for each material group at room temperature, $T = 298.13$ K, and strain rate $\dot{\varepsilon} = 1\ s^{-1}$ .Each group contains $n = 2$ specimens.

Specimen ID	Elastic Modulus (ksi)	Yield Strength (ksi)	UTS (ksi)	Strain Before UTS (%)	Strain After UTS (%)	Total Elongation (%)
RB-R2-1	24814	66.76	83.10	17.05	36.95	54.00
RB-R2-2	24110	66.60	83.01	17.26	34.94	52.20
RB-R3-1	22893	67.52	83.20	16.36	26.30	42.66
RB-R3-2	24262	67.35	82.99	15.94	26.31	42.25
RB-R4-1	22996	69.51	84.88	15.75	35.17	50.92
RB-R4-2	22903	68.68	85.34	15.73	37.97	53.70
RFB-R2-1	23719	68.97	83.89	16.35	33.68	50.03
RFB-R2-2	23874	68.53	83.72	16.67	36.07	52.74
RFB-R3-1	23091	69.57	84.57	14.84	26.08	40.92
RFB-R3-2	23350	69.51	84.33	16.82	24.58	41.40
RFB-R4-1	23900	66.47	84.36	16.31	36.27	52.58
RFB-R4-2	22634	67.35	84.43	17.06	34.57	51.63

MACROSCALE APPROACH

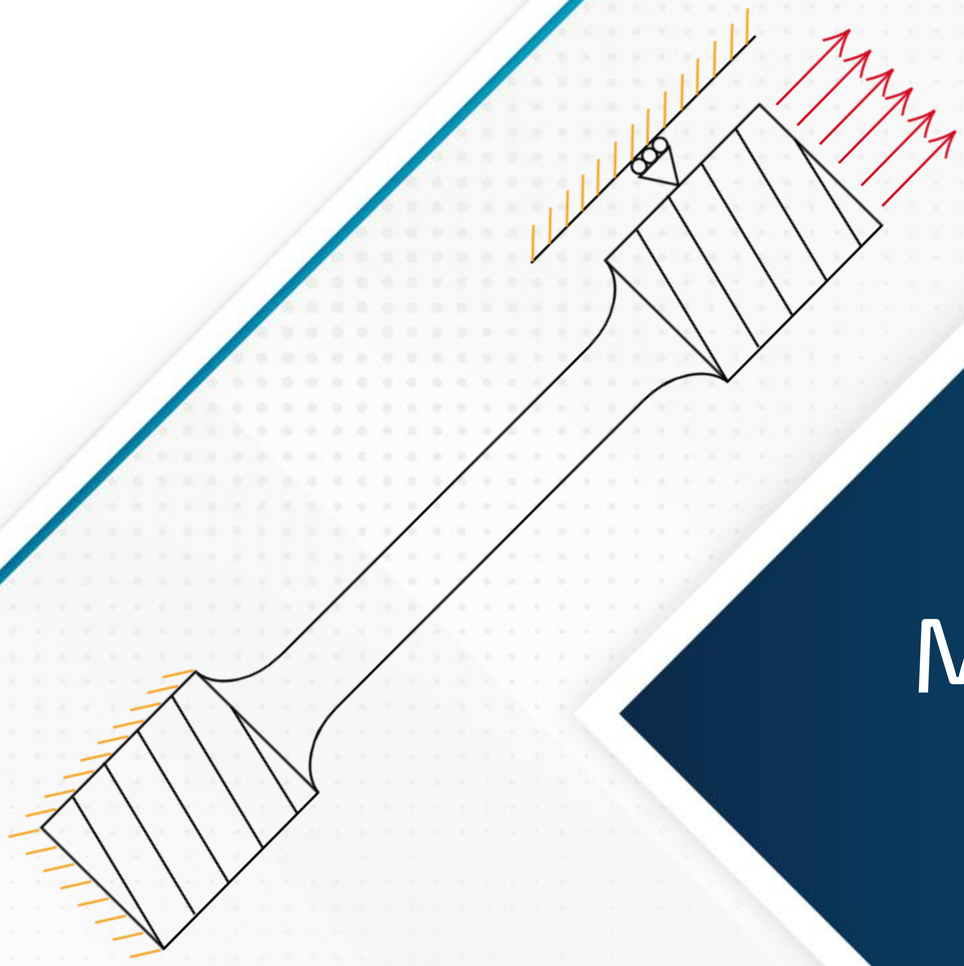

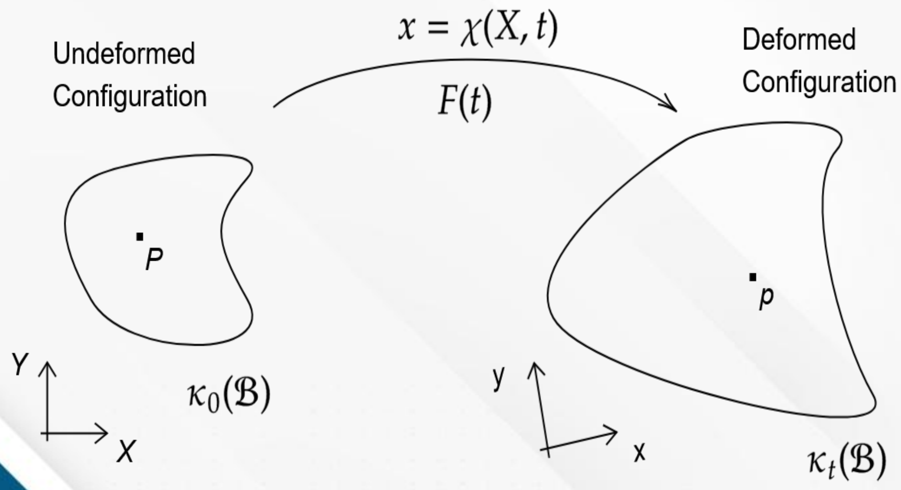

$$\nabla \cdot \sigma^T + \rho f = \rho \left(\frac{\partial v}{\partial t} + v \cdot \nabla v \right)$$

$$0 = \mathcal{F}(E_{ij}, \sigma_{ij}, D_{ij}, \theta, t, \ldots)$$

MACROSCALE MODELS

- Viscoplastic Model [2]
  - Rate-dependent constitutive equation
    - 12 parameters
  - No material degradation
    - Avoid element death for physical meaning

Limitation: Loading in one direction

Rate of Deformation $D = D^e + D^{in}$

Stress rate (objective) only function of elastic rate $\dot{\sigma}_{ij} = \mathbb{C}_{ijkl} D^e_{kl}$

Evolution of the rate of inelastic deformation $D^{in}_{ij} = \frac{3}{2}\gamma(\sigma_{ij}, \theta;\ D, B_{ij})\, n_{ij}$

Flow law for inelastic strain rate $\gamma = f(\theta)\left[\sinh\left(\frac{\tau}{\alpha(\theta)D}\right)\right]^{p(\theta)}$

Evolution Equations

$$\begin{cases} \dot{D} = \dfrac{A_1}{(D - D_0)^{A_3}}\gamma - A_2(D - D_0)^2 \\ \dot{B}_{ij} = \dfrac{A_4}{b^{A_6}} D^{in}_{ij} - A_5 b B_{ij} \end{cases}$$

- UCP Damage Model [3]
  - Viscoplastic model with Wilkens Damage
    - 6 additional parameters
  - Damage scaled by stress state
    - Based on accumulated plastic strain

Limitation: Loading in tension only

Flow law for inelastic strain rate $\gamma = f(\theta)\left[\sinh\left(\frac{\tau}{\alpha(\theta)D(1 - cw^d)}\right)\right]^{p(\theta)}$

Wilkens Damage $w = \int \left(\frac{1}{1 + \frac{p}{\hat{p}}}\right)^{\hat{\alpha}} (2 - A)^{\hat{\beta}}\, d\gamma$

$$w = \int d\gamma$$

MATERIAL CALIBRATION (MATCAL)

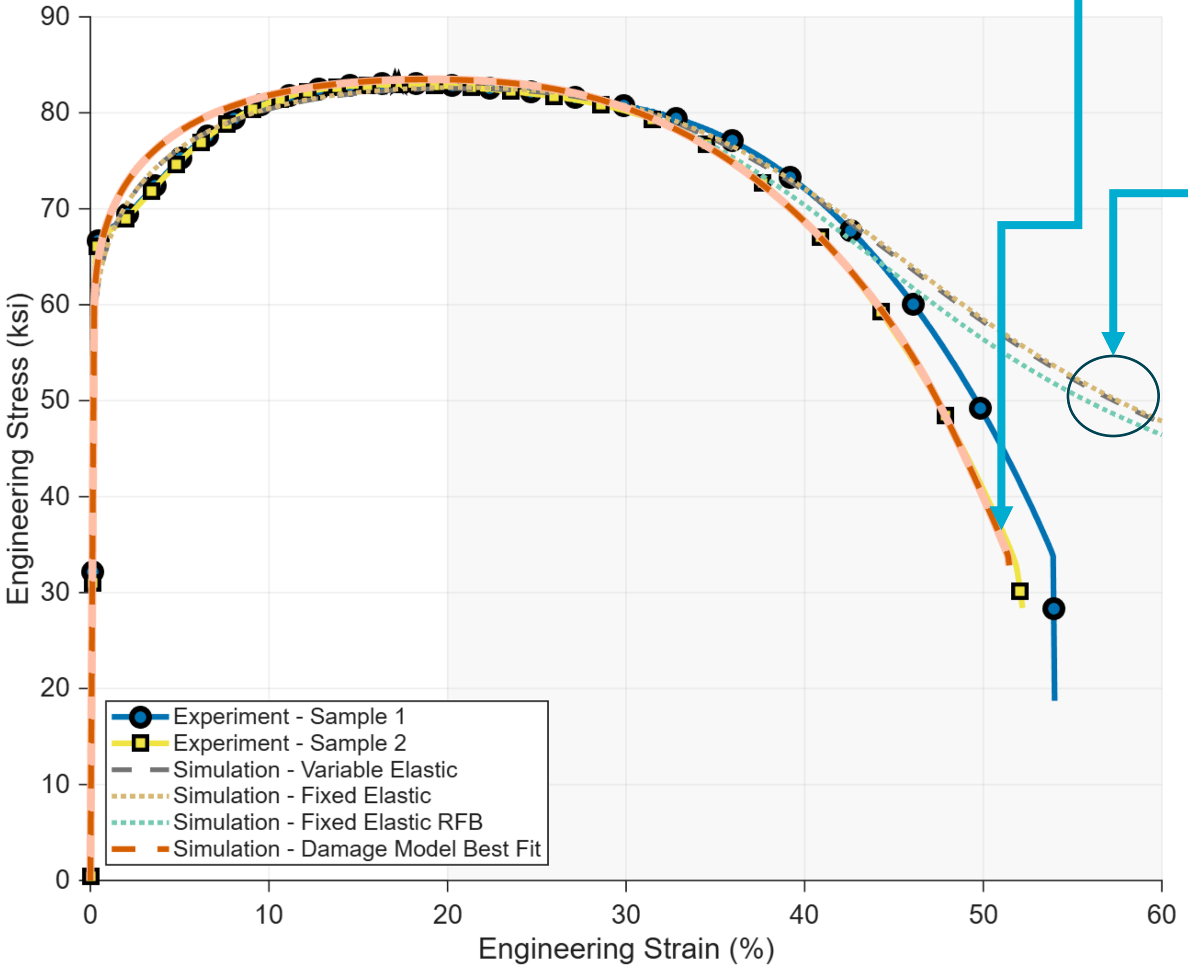

Fig. 2. Progression of material calibration for RB-R2 material group.

Phase 1: Viscoplastic

- Variable elasticity fit
- Fixed elasticity fit [4]
- Single Viscoplastic fit (RFB_R2)

Phase 2: UCP Fail

- Viscoplastic + damage fit

Specimen ID	Damage Effect (*Magnitude*)	Damage Exponent (*Nonlinearity*)	EQPS Fail (*Amount*)
RB-R2-1	0.12	5.00	1.40
RB-R3-1	0.35	2.70	1.20
RB-R4-1	0.08	6.5	1.45
RFB-R2-1	0.17	4.5	1.40
RFB-R3-1	0.40	2.70	1.20
RFB-R4-1	0.07	6.5	1.40

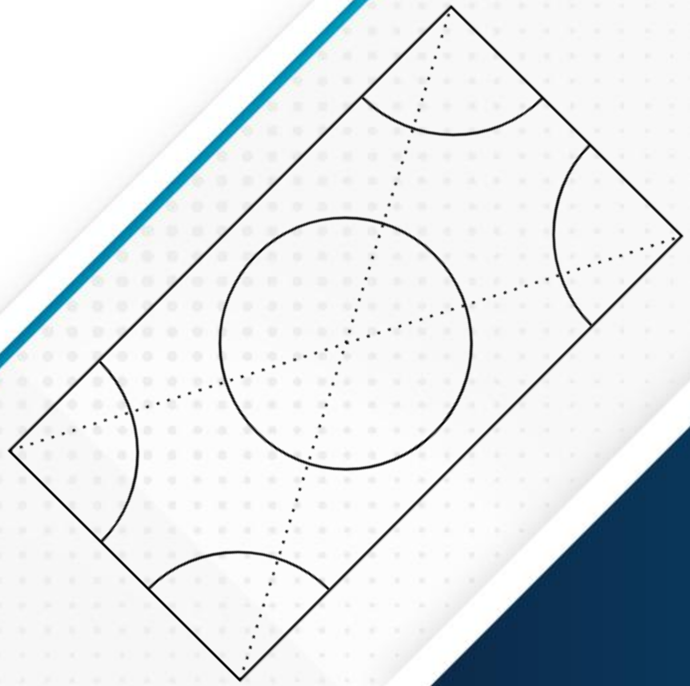

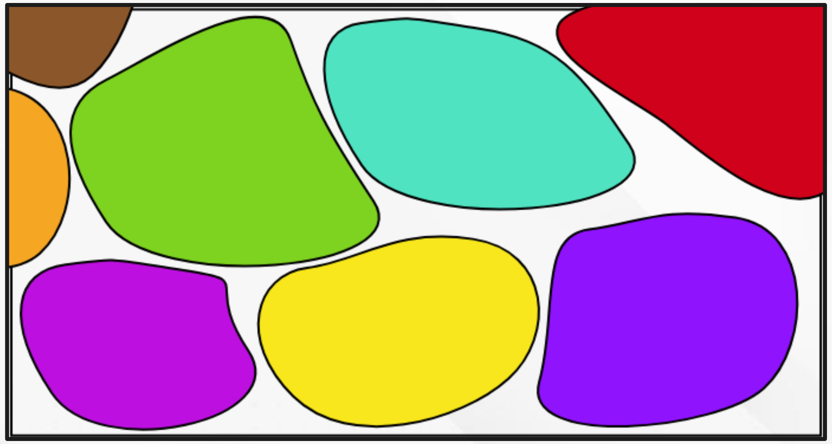

MESOSCALE APPROACH

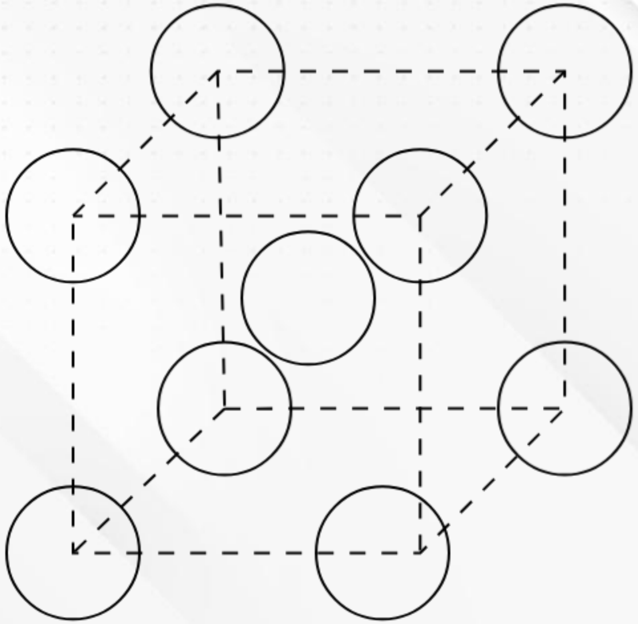

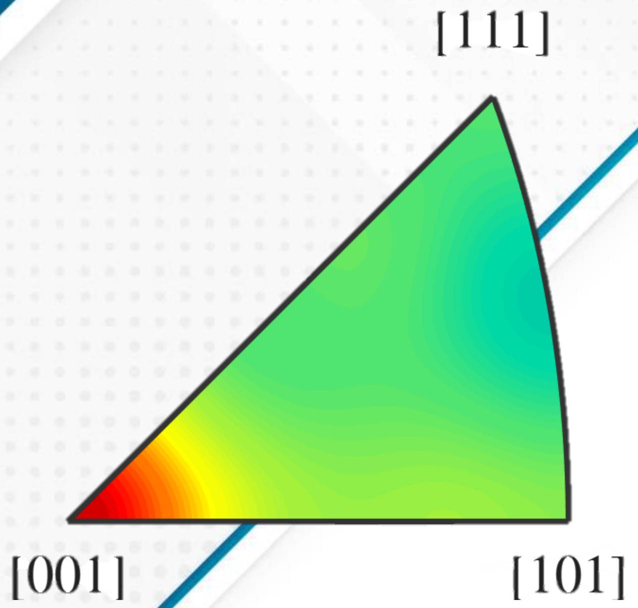

EBSD DATA ANALYSIS

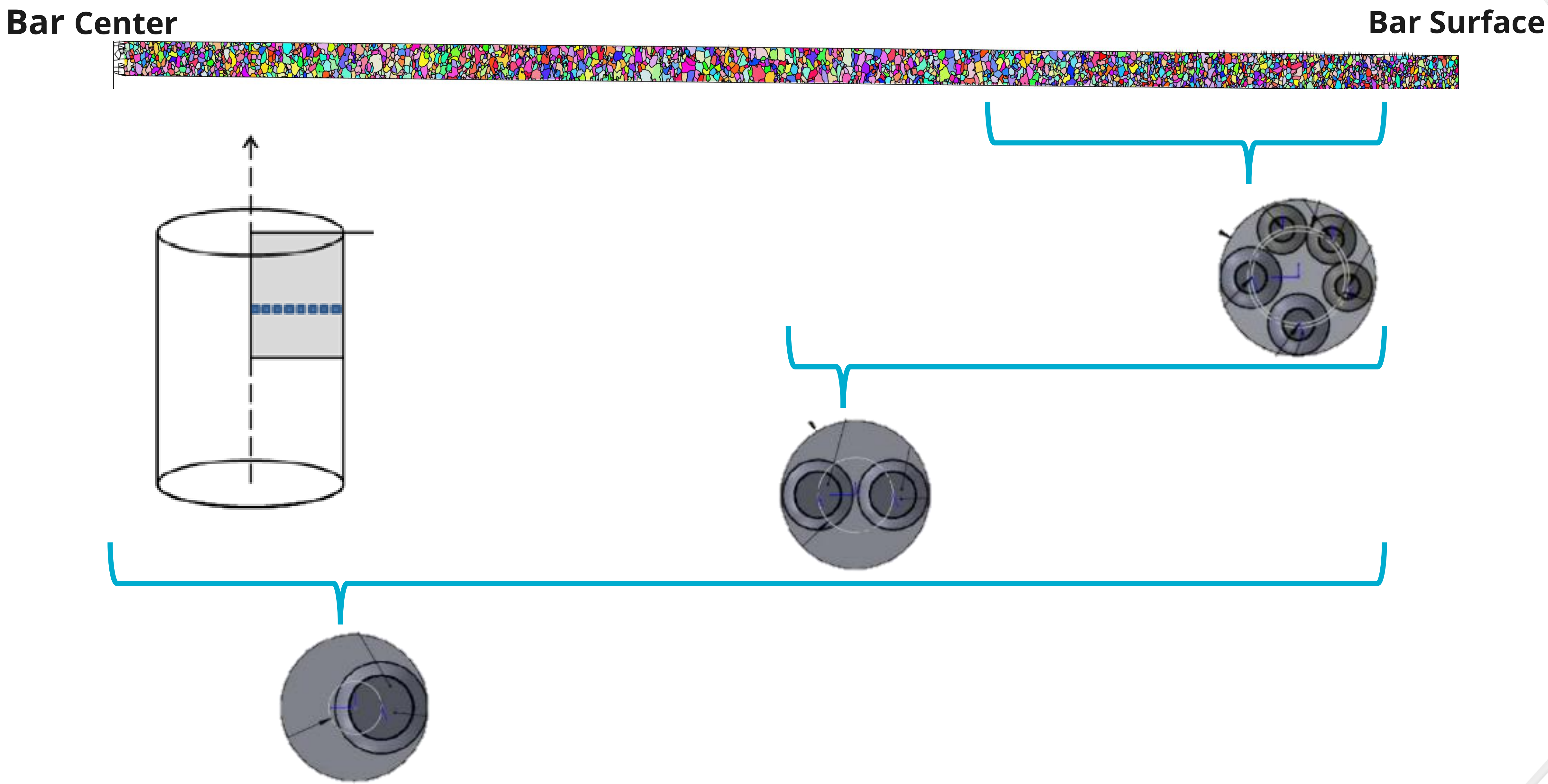

EBSD DATA ANALYSIS

Bar Center

Bar Surface

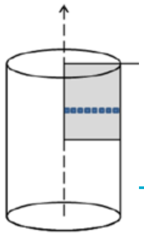

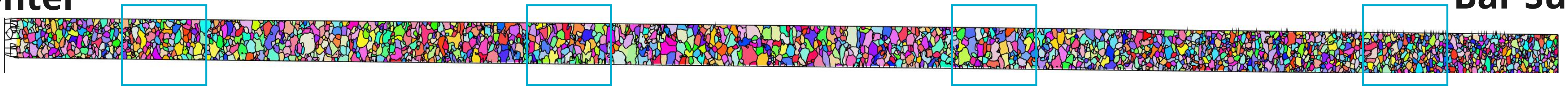

Subsection 1 Subsection 2 Subsection 3 Subsection 4

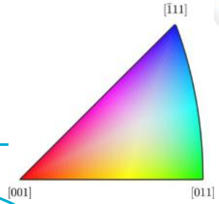

Subsection 1

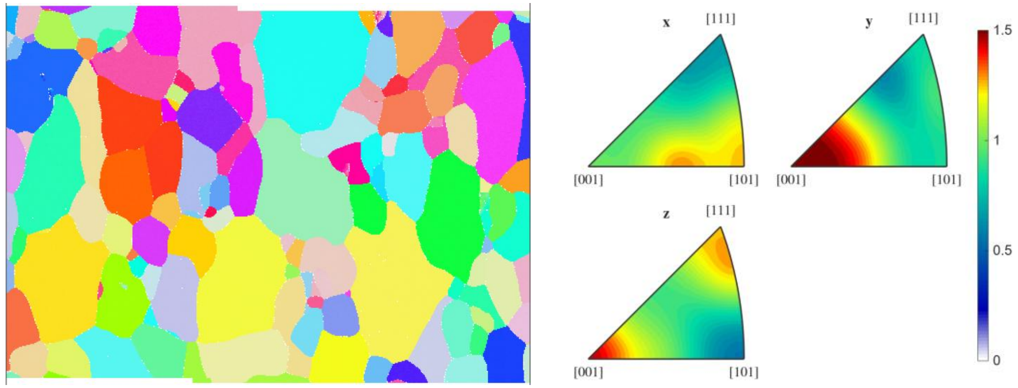

Subsection 2

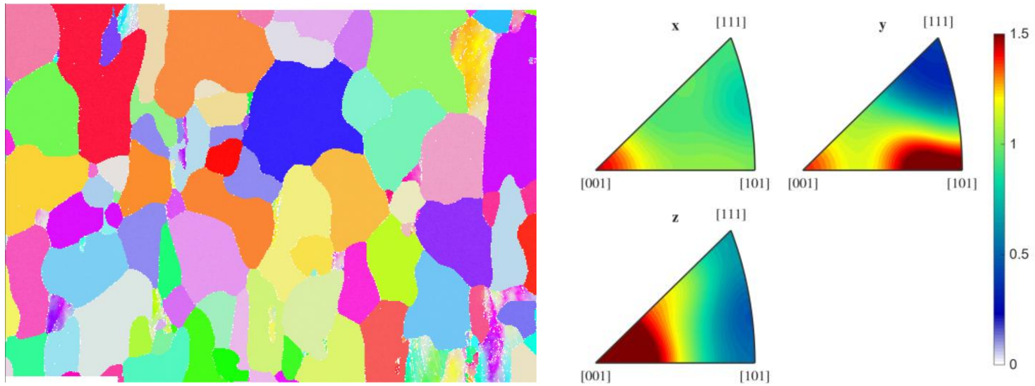

Subsection 3

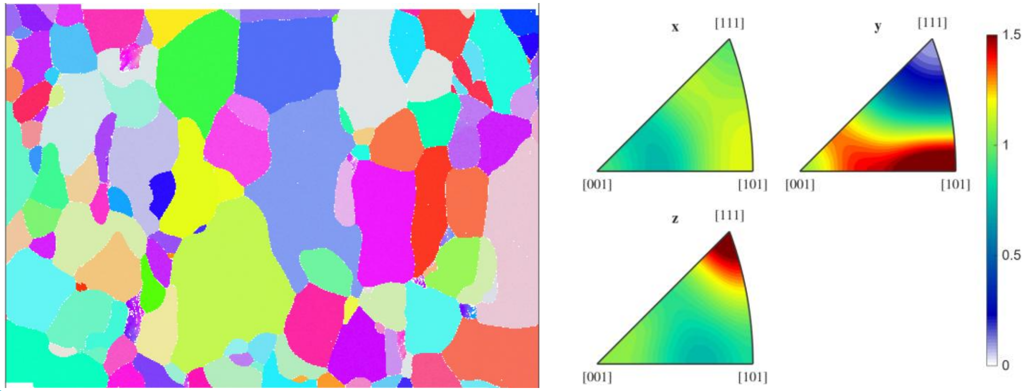

Subsection 4

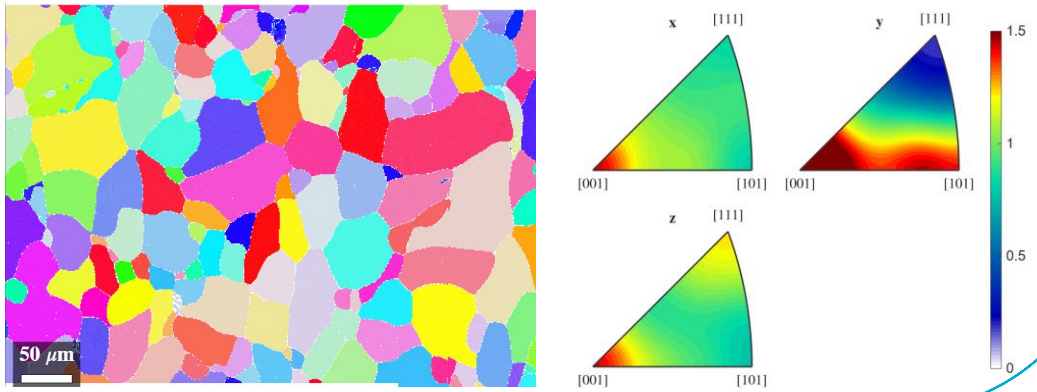

MESH CONSTRUCTION

Bar Center

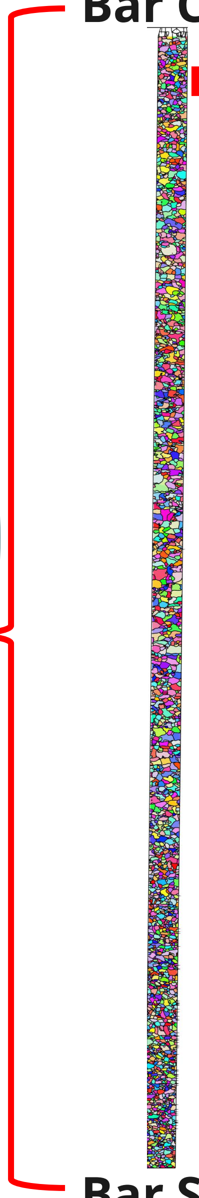

Bar Surface

Bar Long Axis

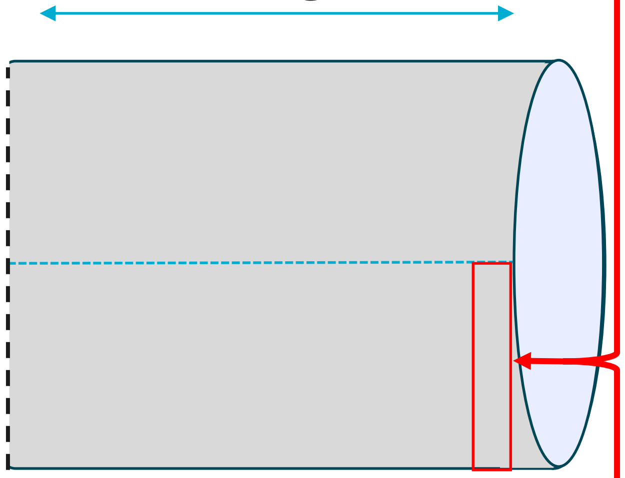

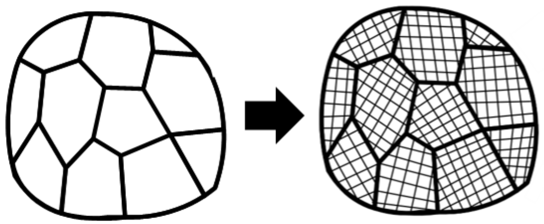

Euler Angles:

- Rotation 1: ϕ_1
- Rotation 2: Φ
- Rotation 3: ϕ_2

$$\mathbf{v}_{\mathbf{global}} = g^{-1}\mathbf{v}_{\mathbf{crystal}}$$

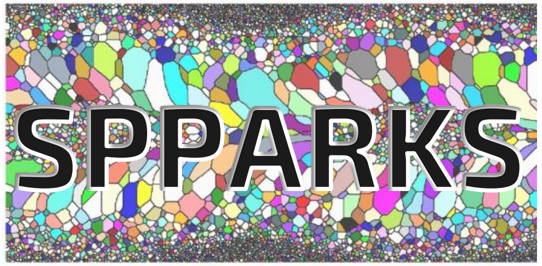

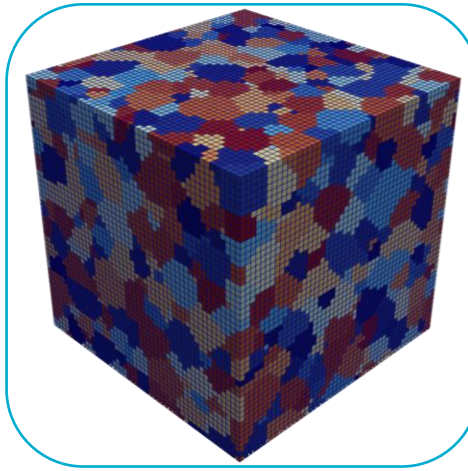

EBSD Data

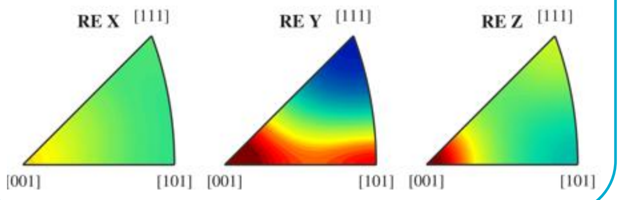

=

Mesh Validation

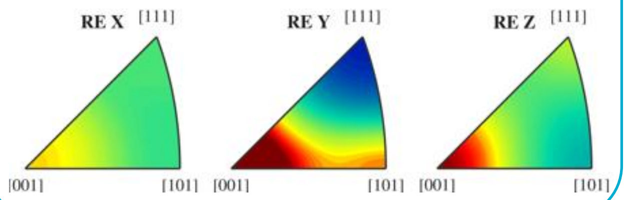

FEA ANALYSIS & MATCAL CALIBRATION

Crystal Plasticity (CP) model

$$\dot{\gamma}^{\alpha} = \dot{\gamma}_0 \left| \frac{\tau^{\alpha}}{\kappa^{\alpha}} \right|^{m} \operatorname{sign}(\tau^{\alpha}),$$

$$\dot{\kappa}^{\alpha} = H \left(\sum_{\beta} q_{\alpha\beta} \left| \dot{\gamma}^{\beta} \right| \right) \left(\frac{\kappa_s - \kappa^{\alpha}}{\kappa_s - \kappa_0} \right),$$

$$\kappa_s = \kappa_{s0} \left(\frac{\sum_{\beta} \left| \dot{\gamma}^{\beta} \right|}{\dot{\gamma}_0} \right)^{n}.$$

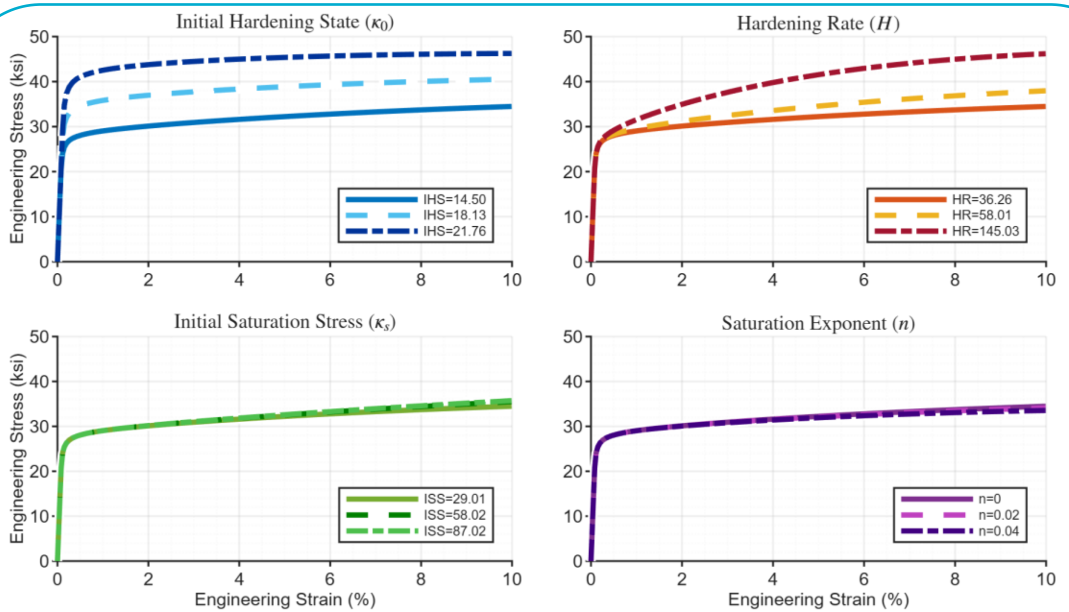

Fig. 3. CP model sensitivity analysis.

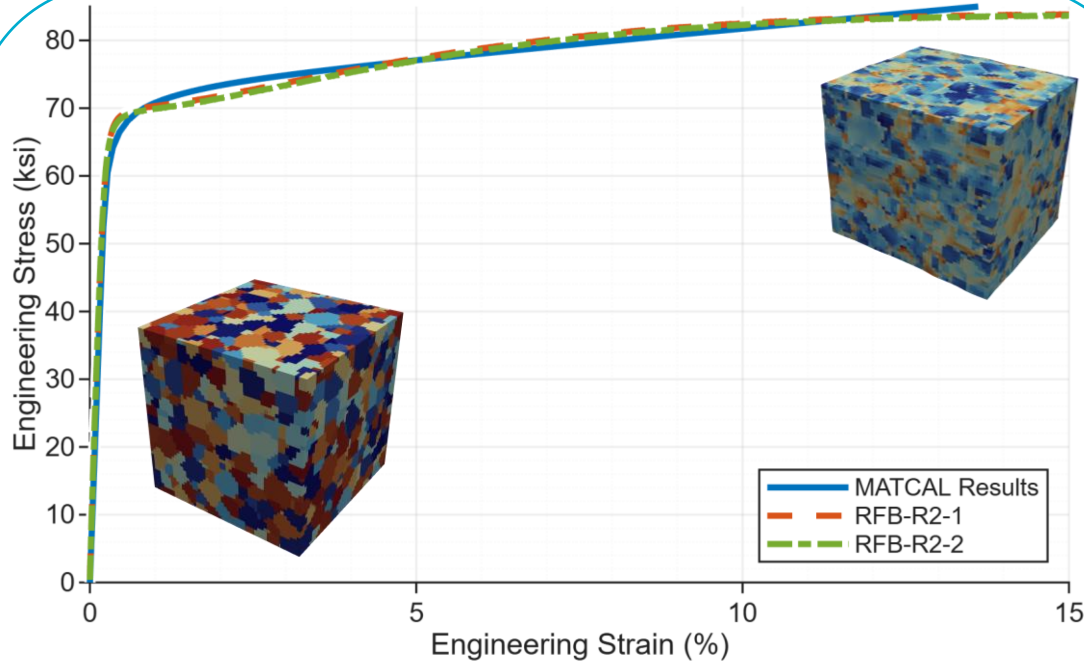

Fig. 4. MATCAL Calibration results for RFB-R2 material group up to UTS for CP model.

Calibrated Parameters up to UTS:

κ_0 (ksi)	H (ksi)	κ_{s0} (ksi)	n
36.62	50.35	0.1450	0.01

LOCAL MICROSTRUCTURE SIMULATION RESULTS & COMPARISON

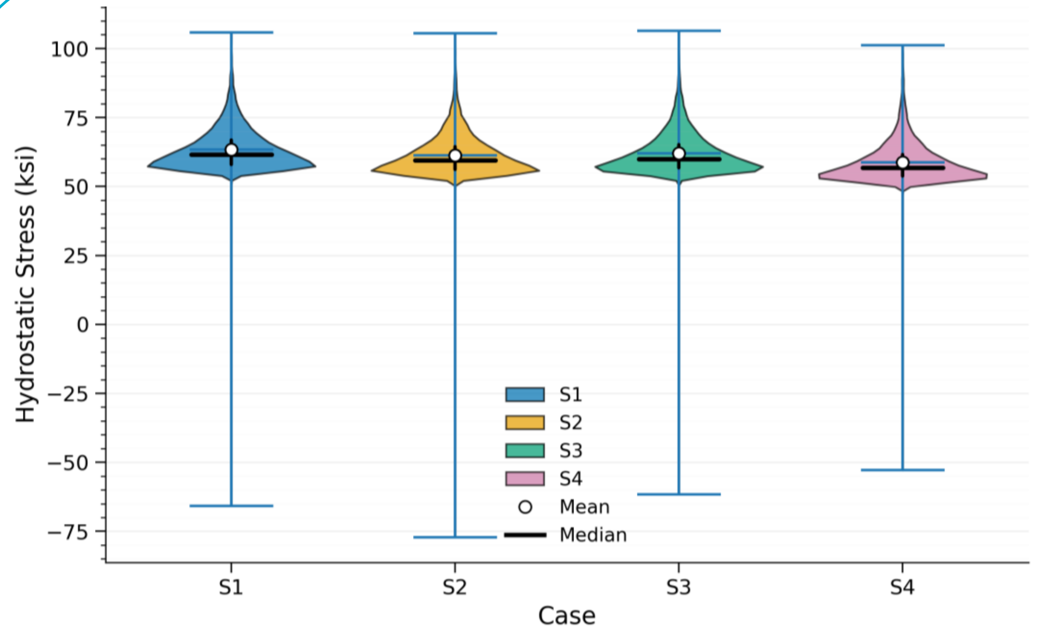

Fig. 5. Violin plot showing density distribution of hydrostatic stress for top 5% absolute maximum at final timestep.

Equation:

$$\sigma_{\mathrm{h}} = \frac{1}{3}\mathrm{tr}(\boldsymbol{\sigma})$$

Meaning:

- Hydrostatic stress promotes **void opening** and **growth**.

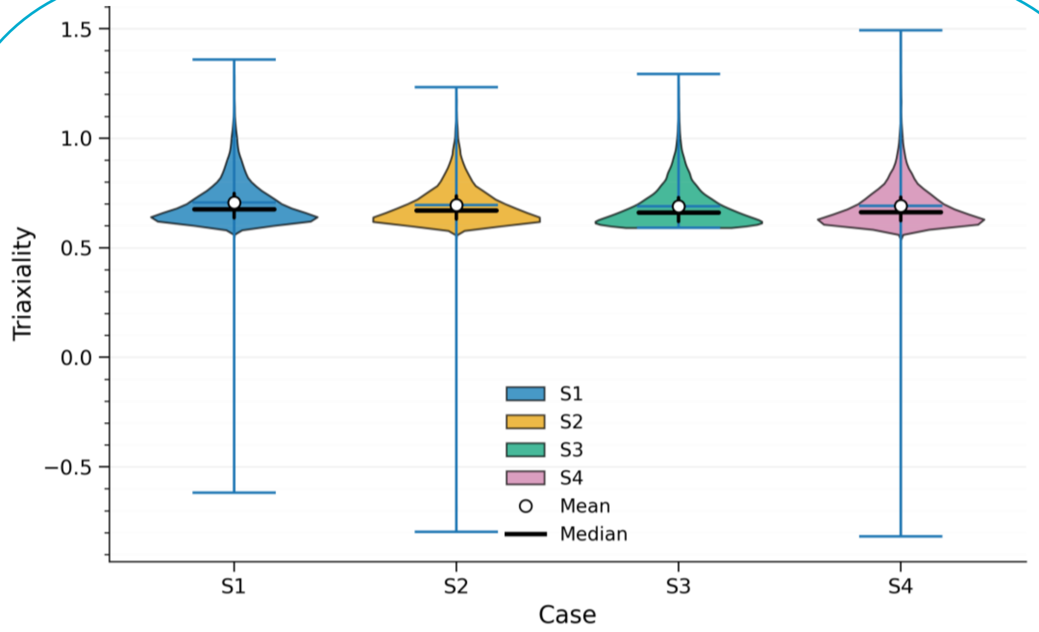

Fig. 6. Violin plot showing density distribution of triaxiality for top 5% absolute maximum at final timestep.

Equation:

$$\eta = \frac{\sigma_{\mathrm{h}}}{\sigma_{\mathrm{vm}}}$$

Meaning:

- Indicates tensile constraint driving **void growth** and **ductile fracture.**

LOCAL MICROSTRUCTURE SIMULATION RESULTS & COMPARISON

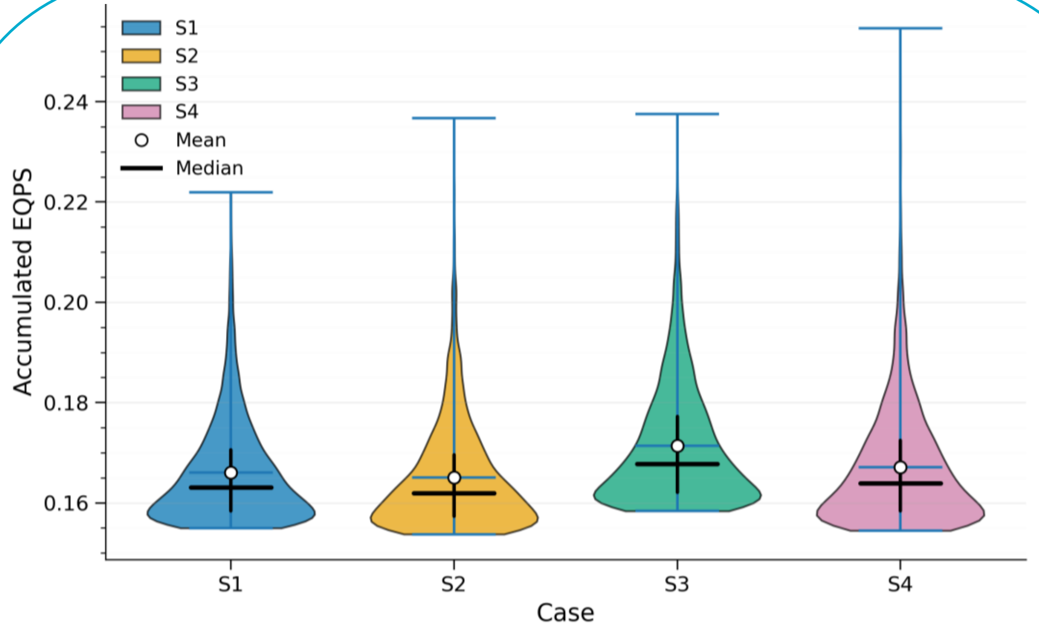

Fig. 7. Violin plot showing density distribution of accumulated EQPS for top 5% absolute maximum at final timestep.

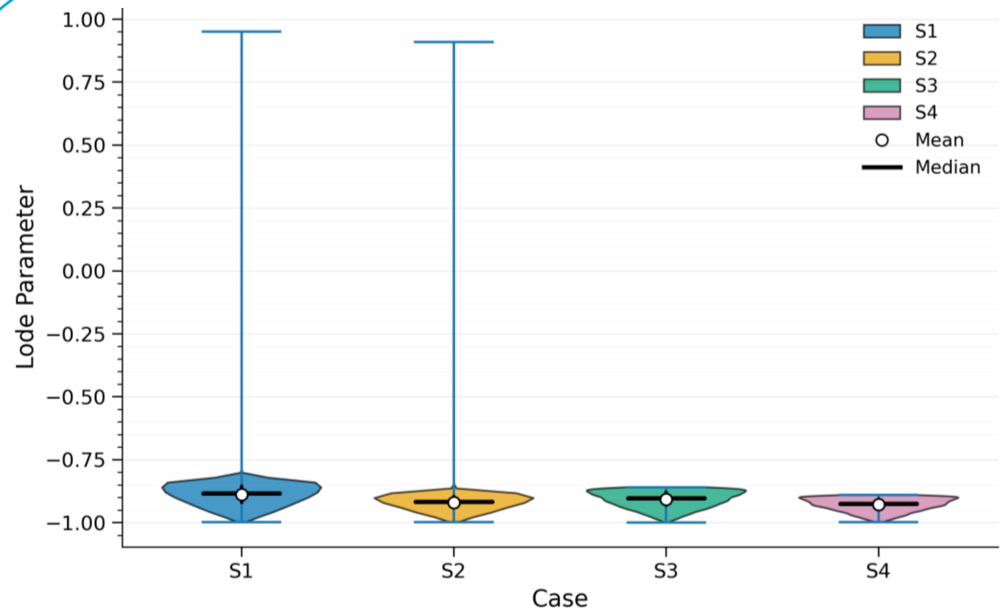

Fig. 8. Violin plot showing density distribution of lode parameter for top 5% absolute maximum at final timestep.

Equation:

$$\varepsilon_{eq}^{\mathrm{in}} = \sqrt{\frac{2}{3}\mathrm{D}^{\mathrm{in}}:\mathrm{D}^{\mathrm{in}}}$$

Meaning:

- Accumulated plastic deformation required for **damage initiation and growth**.

Equation:

$$\mu_{\mathrm{L}} = \frac{2\sigma_2 - \sigma_1 - \sigma_3}{\sigma_1 - \sigma_3}$$

Meaning:

- Distinguishes stress states that affect **fracture mode**.

OUTCOMES

- **R3 specimens showed reduced total elongation** compared with R2 and R4.
- **Yield strength and UTS remained similar** across specimen groups.
- A **viscoplastic-damage continuum model** is needed to capture post-UTS softening and failure.
- Investigated the roles of **damage measures** in failure initiation & propagation before UTS.

CONCLUSIONS/FUTURE DIRECTIONS

- EQPS as the central damage measure to compare macro- and mesoscale.
- Relating parameters to physical mechanism:
  - Incorporate **damage mechanisms** into the crystal plasticity model.
  - Relate damage parameters to void nucleation, growth, and coalescence.
- Investigate **additional stress states**:
  - compression, shear, torsion, multiaxial loading.

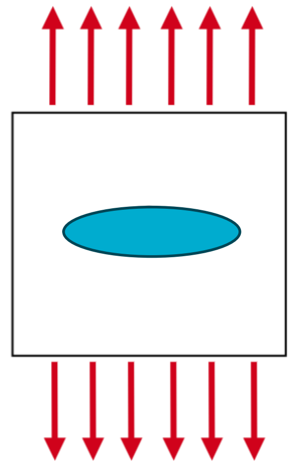

ACKNOWLEDGEMENTS

- This research was conducted at the 2026 Nonlinear Mechanics and Dynamics Research Institute hosted by Sandia National Laboratories and the University of New Mexico.
- Sandia National Laboratories is a multimission laboratory managed and operated by National Technology and Engineering Solutions of Sandia, LLC, a wholly owned subsidiary of Honeywell International, Inc., for the U.S. Department of Energy's National Nuclear Security Administration under contract DE-NA-0003525.

REFERENCES

- [1] A. F. Bower, *Applied Mechanics of Solids*. 2nd ed. Boca Raton, FL, USA: CRC Press, 2025.
- [2] M. K. Neilsen, S. N. Burchett, C. M. Stone, and J. J. Stephens, “A viscoplastic theory for braze alloys,” Sandia National Laboratories, Albuquerque, NM, USA, 1996, doi: 10.2172/233338.
- [3] K. Dion and M. K. Neilsen, “Coupled thermal stress simulations of ductile tearing,” Int. J. Fract., vol. 198, pp. 167–178, 2016, doi: 10.1007/s10704-016-0093-y.
- [4] ASM International, “Tantalum and tantalum alloys,” in ASM Handbook, vol. 2, Properties and Selection: Nonferrous Alloys and Special-Purpose Materials. Materials Park, OH, USA: ASM International, 1990.
- [5] H. Lim, R. Dingreville, L. A. Deibler, T. E. Buchheit, and C. C. Battaile, “Investigation of grain-scale microstructural variability in tantalum using crystal plasticity-finite element simulations,” Comput. Mater. Sci., 2016.
- [6] S. R. Kalidindi, C. A. Bronkhorst, and L. Anand, “Crystallographic texture evolution in bulk deformation processing of FCC metals,” J. Mech. Phys. Solids, vol. 40, no. 3, pp. 537–569, 1992, doi: 10.1016/0022-5096(92)80003-9.
- [7] Y. Bao and T. Wierzbicki, “On fracture locus in the equivalent strain and stress triaxiality space,” Int. J. Mech. Sci., vol. 46, no. 1, pp. 81–98, 2004, doi: 10.1016/j.ijmecsci.2004.02.006.
- [8] C. Ticknor, H. Lim, and P. Noell, “Identification of mechanisms driving heterogeneous void growth in ductile aluminum,” J. Mat. Sci.: Mat. Theory, vol. 10, no.2, 2026, doi: 10.1186/s41313-026-00073-9.

Q&A

TEXAS A&M UNIVERSITY

Abdelrahman Atef Youssef
Ph.D. Candidate

UW

Grant Litynski
Ph.D. in progress